DESIGN CONSIDERATIONS FOR SURVEYOR GUIDANCE[1]

R.K. Cheng[2], C.M. Meredith[3], and D.A. Conrad[4]

Hughes Aircraft Company
Space Systems Division
El Segundo, California

ABSTRACT 13202

The Surveyor lunar soft landing spacecraft will provide preliminary unmanned scientific exploration of the surface of the moon. This paper contains discussion of the pertinent design considerations for midcourse guidance and the terminal descent system. Design of the terminal descent encompasses (1) calculation of fuel requirements based on sensor and propulsion performance characteristics and (2) implementation of the closed loop control scheme required for the terminal portion of the descent. The midcourse correction is made first to correct miss and then, by taking account of terminal descent system characteristics, to maximize the probability of successful soft landing by an appropriate choice of the maneuver component normal to the critical plane.

---

[1]This work was performed under Contract 950056 with the Jet Propulsion Laboratory, California Institute of Technology, under Contract No. NAS7-100 sponsored by the National Aeronautics and Space Administration. The paper is derived from AIAA papers No. 64-644 and 64-654 presented at the AIAA/ION Astrodynamics Guidance and Control Conference, Los Angeles, Aug. 24-26, 1964.

[2]Associate Manager, Surveyor System Analysis Laboratory

[3]Senior Project Engineer

[4]Senior Staff Engineer

I. MISSION PROFILE

The spacecraft is launched from Cape Kennedy into a 66 hour trans-lunar trajectory. The nominal trajectory is targeted to arrive at a preselected landing site with an acceptable approach velocity and at a time which allows pre- and post-impact observation and command to be carried out from the tracking station at Goldstone, California. After launch, tracking data from the DSIF (Deep Space Instrumentation Facility) network is sent to the Space Flight Operations Facility in Pasadena, Calif. for determination of the injection conditions. A single midcourse correction is made during the first pass over Goldstone to correct miss as well as to establish approach conditions which maximize the probability of a successful terminal descent. This correction is made by a set of three throttlable liquid propellant engines (vernier engines), also used during the terminal descent. Following the midcourse correction, tracking is resumed until several hours prior to initiation of the terminal maneuver. The thrust axis is then aligned with the velocity vector, following which a pulse-type radar marks at a given distance from the lunar surface, thereby triggering ignition of the vernier and then the solid propellant main retro engine.

During main-retro burning, the thrust attitude is held fixed by differential throttling of the vernier engines. An accelerometer switch senses thrust decay prior to retro burnout and triggers the subsequent separation of the main retro case. After separation, a four-beam altimeter-doppler radar system, known as the RADVS (Radar Altimeter Doppler Velocity Sensor) begins search to acquire the velocity vector and the range along the thrust axis to

the lunar surface. Simultaneously, the thrust acceleration is reduced to the minimum value of 0.9 lunar g, sensed by a longitudinal accelerometer. After velocity acquisition, the thrust direction is aligned to the velocity vector, establishing a gravity turn for the remainder of the descent. After range acquisition, a velocity error signal is generated by comparing the measured velocity along the thrust axis with the desired velocity, a simple nonlinear function of the measured range, which will be referred to as the "Descent Contour." The measured velocity is initially lower than the corresponding value on the contour, and the thrust acceleration remains at 0.9 g. Near the descent contour, the thrust increases, and the actual range-velocity profile closely follows the contour until a velocity of 10 ft./sec. is reached near 50 ft. altitude. The vehicle attitude, nearly vertical at this time due to the effect of the gravity turn, goes into inertial hold and a desired descent velocity of five feet per second is commanded. About 13 ft. above the surface, the vernier engines are cut off; and the spacecraft falls to the surface, landing with a velocity near 13 ft./sec.

II. SYSTEM REQUIREMENTS AND CONSTRAINTS

The approach geometry is shown in Fig. 1. The system will accommodate approach trajectories which deviate from the vertical by an angle ψ up to 45 deg. For 66-hour trajectories, the normal impact point P_1 is near the equator in the vicinity of 40 deg. west longitude. The ratio of the central angle γ (see Fig. 1) to the approach flight path ζ is about 1.4, giving landing capability over most of the western sector of the visible hemisphere, as well as a portion of the eastern sector.

To keep the arrival time within the Goldstone visibility windows, the system must be designed to accommodate a variation in arrival velocities, characterized by the velocity V_i of an unbraked vehicle at impact. Fig. 2 shows the relation between Goldstone visibility and arrival velocity for a particular launch day. The truncated sinusoid shows the elevation of the moon above the horizon at Goldstone versus Greenwich mean time (GMT). Allowing 5 deg. for local terrain clearance, plus 60 min. for prelanding and 180 min. for post-landing operations, leaves the arrival window shown. The upper two curves show the corresponding unbraked impact velocity as a function of arrival time for the limiting permissible values of launch azimuth. These latter restrictions arise from range safety and instrumentation considerations. The resulting range of arrival velocities which must be considered from the trajectory point of view lie between points B and C. However, the terminal descent system may not be able to accommodate this entire range. It will be shown that sensor constraints limit the acceptable range of main retro burnout velocities and that this range must provide not only for variations in

arrival velocity, but also for burnout velocity variations due to weight changes at midcourse.

Fig. 3 shows the important sensor and propulsion constraints on a range-velocity diagram, applicable to the vernier phase of the descent. The equation of the descent parabola is

$$V^2 = 2(a_{max} - g)R \qquad (1)$$

where V is velocity, R slant range to the lunar surface along the velocity vector, g lunar gravity and a_{max} is a thrust acceleration chosen on the basis of vernier engine thrust capability and allowances for attitude control requirements and sensor requirements. For simplicity of mechanization, the line segments shown are used in place of the parabola. To assure sufficient vernier thrust capability to soft-land, the probability of the main retro phase terminating below this contour must be negligibly small.

The doppler portion of the RADVS has acceptable accuracy up to 700 ft/sec, with a range capability of about 50,000 ft. The altimeter portion has a ceiling of 40,000 ft. due to signal-to-noise considerations, and is further limited, due to circuit design characteristics, by the downward sloping line shown. This does not mean, however, that burnout may not occur above the altimeter limits. The altimeter output is not required until the spacecraft is in the vicinity of the descent contour; otherwise, minimum acceleration is automatically commanded.

At low burnout velocities, main retro pointing errors cause large dispersions in the burnout flight path angle. For satisfactory radar operation in the gravity turn mode, this angle must lie within 45 deg. of the vertical and

there is a further restriction on the angles between the radar beams and the velocity vector. It will be seen that these burnout attitude and flight path constraints define a minimum acceptable burnout velocity.

III. ANALYSIS OF THE TERMINAL DESCENT

Burnout Dispersion Analysis

The main retro engine is sized such that burnout will occur within the allowable region defined by sensor and propulsion constraints. It is necessary to provide for the required range of approach velocities, dispersions in engine characteristics, and for vehicle weight variations due to fuel expended in performing the midcourse maneuver.

For a vertical descent, the burnout velocity is given in terms of the ignition velocity V_o and the retro engine characteristic velocity ΔV by

$$V_{BO} = V_o - \Delta V + gt \tag{2}$$

where g is lunar gravity, t is the burning time, and the characteristic velocity is given by

$$\Delta V = c \ln \frac{w_o}{w_{BO}} \tag{3}$$

where w_o and w_{BO} are the vehicle weights at ignition and burnout and c is the exhaust velocity (proportional to specific impulse). For off-vertical cases the situation is described by the vector diagram shown in Fig. 4.

The principal sources of velocity dispersion are imperfect alignment of the vehicle prior to retro ignition and the variability of total impulse. These variations cause dispersions characterized in Fig. 4 by a 99 percent

dispersion ellipsoid. Note that the scale of the figure is exaggerated and that the burnout velocity ranges from 1/10 to 1/40 of the ignition velocity, and the gravity loss gt is of the same order of magnitude. It is seen that alignment error (about one degree) causes large variations in burnout flight path angle, with the situation becoming more severe as the burnout velocity decreases. To avoid violating the burnout attitude and flight path constraints mentioned previously, the minimum allowable nominal burnout velocity must be restricted to about 250 fps in the vertical case and 300 fps for 45-deg approach angles.

The range of burnout velocities due to main retro dispersions[1], turns out to be about 125 fps (3 sigma), largely the result of main retro total impulse uncertainty. Thus, the maximum nominal burnout velocity must be less than 575 fps, based on the radar limit of 700 fps.

For a vertical descent, the burnout altitude is given by

$$h_{BO} = h_o - V_o t + \Delta D - \frac{1}{2} g t^2 \tag{4}$$

where the characteristic distance ΔD is

$$\Delta D = \frac{c^2}{g} \frac{w_o}{T} \left[1 - \left(1 + \frac{\Delta V}{c} \right) e^{-\Delta V / c} \right] \tag{5}$$

and T is the retro engine thrust (assumed constant).

[1] In the terminal descent system design, the midcourse correction is treated as a deterministic quantity. To a particular correction, corresponds a nominal burnout velocity, with dispersions about this value occurring due to retro phase uncertainties.

For off-vertical approaches, a vector diagram similar to Fig. 4 can be used. The principal point of interest is the altitude dispersion, caused chiefly by the variation in the retro engine thrust level due to unpredictable temperature variations. For large off-vertical approaches, thrust vector misalignment also has a significant effect.

A complete analysis of dispersions due to all error sources is given in Ref 1. The result of such an analysis is the 99% dispersion ellipses shown in Fig 3. Once these ellipses are determined,[1] the required burnout altitude, and hence ignition altitude, follows from the requirement that the probability of burning out within the constraints shall be at least 0.99.

Main Retro Sizing

The main retro propellant loading is determined such that for the heaviest possible vehicle (no midcourse correction) approaching at the highest possible velocity, burnout occurs at the highest possible speed, that is, at the radar limit of 700 fps less the 99% dispersion of 125 fps. This policy allows the maximum possible reduction in burnout velocity due to variations in approach speed and midcourse correction. Since the sensitivity of burnout velocity to initial weight is about 6 fps/lb, a 22 lb midcourse correction reduces the nominal burnout velocity from 575 to 443 fps. This leaves 143 fps possible variations in approach velocity before the 300 fps

[1] For Surveyor, the dispersion ellipses are insensitive to the location of the nominal burnout point in the altitude-velocity plane.

limit imposed by burnout attitude constraints is reached. As the required midcourse maneuver is increased, the allowable variation in approach velocity is correspondingly reduced.

The 143 fps variation may not be sufficient to accommodate the required unbraked impact velocity range discussed previously. In that case, ballast may be provided to increase the burnout velocity when the approach velocity is low. Since, for low approach velocities, the required injection energy is low, the booster can handle the additional weight. Furthermore, the ballast is attached to the main retro case, which is ejected; hence, the vernier fuel requirement is not affected.

The main retro ignition altitude is based on the requirement that burnout occur sufficiently above the descent contour (Fig 3) to allow time to align the thrust axis with the velocity vector before the trajectory intersects the contour. A "nominal burnout locus" is thereby established to allow for altitude dispersions plus an alignment time depending on the maximum angle between the flight path and roll axis at burnout.

Vernier Fuel Analysis

The maximum vernier fuel expenditure occurs when the fuel consumed at midcourse is also maximum. The design philosophy chosen is to provide enough fuel that, given a maximum midcourse correction, the probability of not running out is at least 0.99. One way of doing this is to examine the fuel required for points on the 99% dispersion ellipse and to provide enough fuel for the worst case. In addition, dispersions in specific

impulse, mixture ratio and other factors must be provided for. A reasonable approach to this problem is to provide for the nominal fuel consumption[1] plus the root-sum square of the amounts required for the remaining dispersions. The difference between the nominal consumption and that required for descent from the worst point on the dispersion ellipse is treated also in the RSS sense.

Based on such an analysis, vernier fuel requirement curves as shown in Fig. 5 can be determined. These curves indicate the amount of propellant required as a function of midcourse correction and burnout velocity (or unbraked impact velocity). The amount of fuel to be provided corresponds on this figure to the maximum midcourse correction and the maximum unbraked impact velocity. Figure 6 indicates the portion of the total propellant allotted to dispersions. This procedure, although convenient to apply, is based on a substantial simplification of the true statistical problem. In particular, basing requirements on the worst point on a dispersion ellipse seems conservative, since some points outside the ellipse result in less fuel consumption. Also, dispersions due to specific impulse and oxygen-fuel mixture ratio uncertainties depend on the actual fuel burned, which itself is a random variable. To better understand the approximations of the simplified analysis, a Monte-Carlo simulation of the terminal descent

[1] "Nominal" refers to the fuel required to descend from the center of the dispersion ellipse corresponding to a maximum midcourse fuel consumption.

has been developed, which employs a simplified analytical model[1], which, though not accurate enough for all purposes, is adequate for fuel computations. With this model, 1000 descents can be computed in about half a minute, and it becomes feasible to generate the various random quantities individually for each run and directly compute the probability of having enough fuel as a function of the fuel loading. Based on a 99% probability of success, the fuel requirement, based on the Monte Carlo model, is about two pounds less than the corresponding values from Fig. 5, which confirms the adequacy of the more simplified procedure for preliminary work.

Vernier Phase Guidance

The guidance method used during the vernier phase consists of (a) continual alignment of the thrust vector along the velocity vector and (b) thrust acceleration control in accordance with the nominal required velocity versus slant range "descent contour" (Fig 3). The attitude control law (a), a gravity turn, begins after the initial thrust axis pointing error has been corrected. For all acceleration levels, the gravity turn has the desirable property that, as the velocity approaches zero, the flight path and thrust direction approach vertical. The thrust control law (b) insures that the cutoff velocity of 5 ft/sec is reached at the desired terminal altitude.

[1]The procedure described previously uses a precise model of the terminal descent, which requires numerical integration and uses about 30 seconds of computing time (IBM 7094) per run.

For a gravity turn descent in a uniform gravitational field, the equations of motion are

$$\frac{dV}{dt} = -a + g \cos \psi \tag{6}$$

$$V \frac{d\psi}{dt} = -g \sin \psi \tag{7}$$

where V is the magnitude of the velocity vector and ψ the angle it makes with the downward vertical. When the thrust acceleration a is constant, the solution is found by dividing (6) by (7), separating the variables and integrating. The resulting expression relates V and ψ to the initial conditions V_o and ψ_o:

$$\frac{V}{V_o} = \left(\frac{\tan \frac{\psi}{2}}{\tan \frac{\psi_o}{2}} \right)^{\frac{a}{g} - 1} \frac{\sec^2 \frac{\psi}{2}}{\sec^2 \frac{\psi_o}{2}} \tag{8}$$

From (7) and (8) the attitude rate is

$$\frac{d\psi}{dt} = -\frac{g \sin \psi}{V_o} \left(\frac{\tan \frac{\psi_o}{2}}{\tan \frac{\psi}{2}} \right)^{\frac{a}{g} - 1} \frac{\sec^2 \frac{\psi_o}{2}}{\sec^2 \frac{\psi}{2}} \tag{9}$$

If $a/g > 2$, as is the case during the major portion of the descent following the minumum acceleration phase, (9) indicates that $d\psi/dt$ diverges as ψ approaches zero. Since the vehicle turning rate is limited due to finite gyro torquing capability, it is important to have a descent contour which

allows a reduced thrust acceleration (<2g) near the end of the closed loop guidance phase. As will be shown later, this is accomplished by a final straight line segment passing through the origin of the range-velocity plane.

The minimum acceleration (0.9 lunar g) gravity turn starts from a velocity which depends on the main retro characteristic velocity and thrust attitude. This phase terminates at the descent contour with only a small change in velocity. If the initial flight path is nearly vertical, the intersection velocity is slightly higher than the initial because the thrust acceleration is less than one lunar g. If the initial flight path is greater than $\cos^{-1}(a/g)$, the right side of (6) will be negative and the velocity will first decrease until $\psi = \cos^{-1}(a/g)$ and then will gradually increase as ψ approaches zero.

In the vicinity of the descent contour, the thrust acceleration command is proportional to the velocity error, defined as the difference between the measured velocity V_z along the thrusting direction and the required velocity V corresponding to the measured slant range, as shown in Fig. 7. The resulting characteristic relating thrust acceleration command and velocity error contains a linear region, which prevents noise induced chattering between the thrust limits.

The velocity, V_s, of intersection with the descent contour is variable, depending on midcourse and retro dispersions. If intersection occurs close to the upper end of a particular segment (Fig. 3), the acceleration saturates, and the trajectory sags below the segment, returning to it at a lower velocity,

V_a, at which point the acceleration is reduced to the value required to remain on the segment. This acceleration is given approximately by

$$a \approx V \frac{dV}{dR} + g = V \frac{V_2 - V_1}{R_2 - R_1} + g \qquad (10)$$

where subscripts 1 and 2 denote the lower and upper ends of the segment. The velocity V_a depends on V_s and to a lesser extent on the flight path angle ψ_s. In general, the higher the values of V_s and ψ_s, the lower V_a tends to be. A finite tracking period after reacquisition of the segment is desirable to insure that the trajectory develops a similar two-phase characteristic along the following segments. This guarantees that there will subsequently be enough acceleration capability to soft-land. The placement of the end points along the parabolic contour is based, therefore, partly on meeting certain minimum tracking period requirements along each segment. Other considerations in the descent contour design arise from the effects of surface slope, system errors, and radar noise, which also influence the required margin between the upper acceleration limit and the nominal acceleration level.

The final segment and an associated trajectory are shown in Fig. 8. The velocity V_o, at the top of the segment, is low enough so that there is a negligible probability of the minimum acceleration phase terminating on the final segment. For most main-retro burnout conditions, the gravity turn will have reduced the flight path ψ to a small value at P_o, so the subsequent descent can be considered vertical. The acceleration required to remain on

the final segment (or any straight line passing through the origin) is readily shown to be

$$a = V\frac{V_o}{R_o} + g \qquad (11)$$

Hence, the required acceleration approaches one lunar g as the velocity approaches zero. As noted above, this reduction in acceleration to less than 2 lunar g's is required to keep the turning rate within acceptable bounds.

The trajectory along the final segment shows a saturated and then a tracking portion until the velocity reaches the preset value V_b of 10 ft/sec. The required velocity is then switched to the constant value V_c of 5 ft/sec and the vehicle attitude to inertial hold. After point B a short transient occurs during which the acceleration is momentarily saturated; then the acceleration is reduced to one lunar g for a constant velocity descent (5 ft/sec) which compensates for prior altitude errors.

When the measured altitude reaches R_c (presently 13 ft) the engines are shut off and the vehicle falls to the lunar surface, impacting nominally at 12.8 ft/sec, with small errors (about 2 ft/sec), arising from the radar measurements at shut-off.

The landing is nominally vertical; however, horizontal velocity dispersions arise from (1) measurement error in the doppler system resulting in a velocity error normal to the thrust axis, and (2) non-vertical attitude at point B, due to attitude transients and termination of the gravity turn at a finite velocity. Since the attitude at point B is inertially held throughout the remainder of powered descent until cutoff, these error sources can cause a significant lateral velocity at touchdown. The vehicle landing gear must be designed to withstand this velocity without toppling.

IV MIDCOURSE GUIDANCE

A number of midcourse guidance techniques have been presented previously,[2,3] most of which tend to treat only the problem of correcting the trajectory to land at the desired site. If additional terminal considerations are taken into account, it is to the extent of correcting miss and flight time or miss and impact velocity. One discovers, however, that other terminal considerations, such as radar performance limitation, fuel requirement, time available for spacecraft command, and scientific experiments all have a strong influence on overall mission success. Various terminal parameters of interest can be controlled, to a certain extent, by the magnitude and direction of the midcourse correction.

Lunar Miss Coordinates

The lunar miss is specified in terms of the conventional miss parameter, or **B** vector[4], in the **R - S - T** coordinate system (Figure 9). The miss parameter is defined from the center of the moon perpendicular to the incoming asymptote of the lunar approach hyperbola. **T** is defined here as a unit vector which lies along the intersection of the earth's equatorial plane and the plane normal to the asymptote. **R** is a unit vector normal to both **T** and a unit vector **S** along the incoming asymptote. The **B** vector is therefore specified by it's components B_R and B_T in the **R** and **T** directions.

Critical Plane Correction

The effect of a midcourse velocity increment $\Delta \mathbf{V}_m = (\Delta \dot{X}_m, \Delta \dot{Y}_m, \Delta \dot{Z}_m)$ on the miss parameter is given, to first order, by

$$\begin{aligned} \Delta B_T &= \nabla B_T \cdot \Delta \mathbf{V}_m \\ \Delta B_R &= \nabla B_R \cdot \Delta \mathbf{V}_m \end{aligned} \tag{12}$$

where the components of $\Delta \mathbf{V}_m$ are expressed in a rectangular cartesian coordinate system X_m, Y_m, Z_m, and ∇ denotes the gradient with respect to these coordinates.

In the same manner changes in the impact velocity and flight time are given by

$$\begin{aligned} \Delta V_i &= \nabla V_i \cdot \Delta \mathbf{V}_m \\ \Delta T_F &= \nabla T_F \cdot \Delta \mathbf{V}_m \end{aligned}$$

The maximum change in B_T and B_R occurs when $\Delta \mathbf{V}_m$ lies in the plane of ∇B_T and ∇B_R, the so-called critical plane, defined by its unit normal

$$\mathbf{U}_3 = \frac{\nabla B_T \times \nabla B_R}{|\nabla B_T \times \nabla B_R|} \tag{13}$$

A perturbation along $\mathbf{U}_3$ will make no first order change in B_T and B_R. As a result, the direction of $\mathbf{U}_3$ is sometimes called the non-critical direction.

The sense of $\mathbf{U}_3$ is defined such that a positive $\mathbf{U}_3$ component of the midcourse correction causes an increase in flight time.

The critical plane maneuver $\Delta \mathbf{V}_c$ is the minimum correction that will result in a desired ΔB_T and ΔB_R. The required maneuver must satisfy the three equations

$$\begin{aligned} \Delta B_T &= \nabla B_T \cdot \Delta \mathbf{V}_c \\ \Delta B_R &= \nabla B_R \cdot \Delta \mathbf{V}_c \\ 0 &= \mathbf{U}_3 \cdot \Delta \mathbf{V}_c \end{aligned} \tag{14}$$

where the third equation confines the correction to the critical plane. These equations can be written in matrix notation as $\delta \mathbf{B} = \mathbf{K} \Delta \mathbf{V}_c$ where the third component of $\delta \mathbf{B}$ is zero and $\mathbf{K}$ is a 3×3 matrix, inversion of which yields the desired correction

$$\Delta \mathbf{V}_c = \mathbf{K}^{-1} \delta \mathbf{B} \tag{15}$$

To insure that the computation does not degrade the overall guidance accuracy, the final correction is computed by an iterative procedure. The maneuver calculated in Equation (15) is applied to the trajectory program and the residual miss determined. A new correction is then computed:

$$\left[\Delta \mathbf{V}_c \right]_{n+1} = \left[\Delta \mathbf{V}_c \right]_n + \mathbf{K}^{-1} \left[\delta \mathbf{B} \right]_n \quad (n = 1, 2, 3, \ldots)$$

The iteration process is terminated when the residual miss becomes less than some threshold value.

Terminal Considerations

In addition to arriving at the preselected landing site, various other terminal constraints, discussed in Section II, must be satisfied for successful completion of the mission. Those of particular interest to the midcourse maneuver are (1) the minimum main retro burnout velocity, (2) the maximum burnout velocity, (3) latest allowable arrival time, (4) earliest allowable arrival time and (5) vernier engine propellant constraints.

It follows, from the definition of the non-critical direction, that the component V_n of the midcourse correction along $\mathbf{U}_3$ can be varied to satisfy the aforementioned terminal constraints without affecting, to a first approximation, the landing site. The values of V_n that will just satisfy the maximum and minimum main retro burnout velocities are found as follows. It can be shown that the main retro burnout velocity V_{BO} is a function of the unbraked impact velocity V_i, the unbraked impact angle γ_i, and the spacecraft weight at main retro ignition W_o

$$V_{BO} = f(V_i, \gamma_i, W_o)$$

This relationship can be approximated over a wide range by the expansion

$$V_{BO} = V_{BO_r} + \frac{\partial V_{BO}}{\partial V_i}\left[V_i - V_{i_r}\right] + \frac{\partial V_{BO}}{\partial W_o}\left[W_o - W_{o_r}\right] \qquad (16)$$

where the subscript r denotes the reference conditions. It should be noted that γ_i remains relatively fixed for a particular landing site. The ignition weight and impact velocity in (16) are given by

$$W_o = W_s \left[1 - \frac{|\Delta \mathbf{V}_c + V_n \mathbf{U}_3|}{c} \right] = W_s - W_m \tag{17}$$

$$V_i = V_{i_o} + \nabla V_i \cdot (\Delta \mathbf{V}_c + V_n \mathbf{U}_3) \tag{18}$$

where W_s is the pre-midcourse spacecraft weight, W_m the propellant used at midcourse, c the vernier engine exhaust velocity and V_{i_o} is the uncorrected impact velocity. Inserting (17) and (18) in (16) leads to an implicit relation between V_n and V_{BO}:

$$V_n = A_4 + A_3 \left[|\Delta \mathbf{V}_c|^2 + V_n^2 \right]^{1/2} \tag{19}$$

where A_3 and A_4 depend on V_{BO} and the various other constants appearing in (16), (17) and (18).

Squaring (19) leads to a quadratic in V_n to be solved at the maximum and minimum main retro burnout velocities $V_{BO_{max}}$ and $V_{BO_{min}}$. Denoting the two values of V_n that satisfy (19), for $V_{BO} = V_{BO_{min}}$ by V_1 and V_2, then any value of V_n such that

$$\min (V_1, V_2) < V_n < \max (V_1, V_2)$$

will satisfy the minimum main retro burnout velocity constraint.

If solutions for (19) exist at $V_{BO} = V_{BO_{max}}$, and these solutions are denoted by V_3 and V_4, all values of V_n such that

$$\min (V_3, V_4) < V_n < \max (V_3, V_4)$$

will violate the maximum main retro burnout velocity constraint.

The velocities in the non-critical direction that will just satisfy the arrival time constraints are given by

$$V_n T_1 = \frac{T_{min} - T_{F_o} - (\nabla T_F \cdot \Delta \mathbf{V}_c)}{\nabla T_F \cdot \mathbf{U}_3} \tag{20}$$

$$V_n T_2 = \frac{T_{max} - T_{F_o} - (\nabla T_F \cdot \Delta \mathbf{V}_c)}{\nabla T_F \cdot \quad 3} \tag{21}$$

where T_{F_o} is the uncorrected flight time and T_{max} and T_{min} are flight times corresponding to the maximum and minimum arrival times.

The maximum allowable correction in the non-critical direction is

$$V_{n_{max}} = \left[V^2_{max} - |\Delta \mathbf{V}_c|^2 \right]^{1/2} \tag{22}$$

where V_{max} is determined by the maximum amount of propellant available for the midcourse correction.

The problem is reduced to one of holding the component of the maneuver in the critical plane fixed while varying the component along the non-critical direction. The existence of a possible maneuver depends upon the existence of

a finite interval, or intervals, defined by the required maneuver to satisfy the constraints. There are three possibilities, as shown in Figure 10, where

$$A = \max \left[- V_{n_{max}}, \min (V_1, V_2), V_n T_1 \right]$$

$$B = \min \left[V_{n_{max}}, \max (V_1, V_2), V_n T_2 \right]$$

First, for an interval to exist, B must be greater than A; second, if there are no roots V_3 and V_4, the interval is from A to B; otherwise, let $C = \min [V_3, V_4]$ and $D = \max [V_3, V_4]$, and the interval is from A to C if $A < C \leq B$ and/or from D to B if $A \leq D < B$. If an interval, or intervals, can be found that satisfy the above constraints, it/they will be explored for the "optimum" component in the non-critical direction.

Propellant Considerations

The critical plane correction is the minimum maneuver required to correct a given miss, but in studying the combined midcourse and terminal systems one discovers that the critical plane correction is not the optimum from an overall fuel standpoint. The fuel margin FM can be defined as the residual vernier engine propellant after subtracting the amount required for the midcourse correction W_m and the nominal terminal descent W_T

$$FM = W_{f_o} - W_m - W_T \tag{23}$$

where W_{f_o} is the weight of the tanked propellant.

For a given change in the non-critical component of the midcourse maneuver, the change in the fuel margin is given by

$$\frac{dFM}{dV_n} = - \frac{dW_m}{dV_n} - \frac{\partial W_T}{\partial V_i} \frac{dV_i}{dV_n} - \frac{\partial W_T}{\partial W_o} \frac{dW_o}{dV_n}$$

since $W_o = W_s - W_m$

$$\frac{dFM}{dV_n} = \left[\frac{\partial W_T}{\partial W_o} - 1 \right] \frac{dW_m}{dV_n} - \frac{\partial W_T}{\partial V_i} \frac{dV_i}{dV_n}$$

From Equation (17)

$$\frac{dW_m}{dV_n} = \frac{W_s/c}{[(|\Delta \mathbf{V}_c|/V_n)^2 + 1]}$$

and

$$\frac{dV_i}{dV_n} = \nabla V_i \cdot \mathbf{U}_3$$

The ∇V_i is a function of the midcourse maneuver time while $\partial W_T/\partial V_i$ and $\partial W_T/\partial W_o$ are dependent upon the particular propellant loading. Setting the derivative to zero and letting

$$B_1 = \left[\frac{\partial W_T}{\partial W_o} - 1 \right] \frac{W_s}{c}$$

$$B_2 = \frac{\partial W_T}{\partial V_i} (\nabla V_i \cdot \mathbf{U}_3)$$

gives the optimum V_n from propellant considerations

$$V_n = \frac{|\Delta V_c|}{[(B_1/B_2)^2 - 1]^{1/2}} \tag{24}$$

For the Surveyor spacecraft, with a midcourse correction 15 hours after injection, Equation (24) becomes

$$V_n = \frac{\Delta V_c}{1.1}$$

In any case, a component of the midcourse maneuver in the non-critical direction can be utilized to reduce both the unbraked impact velocity and spacecraft weight. This in turn will reduce the vernier propellant requirement for the terminal descent phase. Therefore, in certain instances, by increasing the fuel used at midcourse the overall vernier engine fuel margin can be increased, thereby increasing the propellant available for terminal descent dispersions and the probability of a successful soft landing. The fuel margin should not be increased, however, at the expense of other terminal considerations.

Midcourse Value Factor

It is difficult to formulate a simple analytic method to find the overall "optimum" V_n. A simple search method has been designed that results in a good compromise between the various parameters over a wide range of injection conditions. Three weighting functions are defined (Figures 11, 12 and 13) which reflect the probability of satisfying the mission requirements for each of the

constraining variables (i.e., radar constraints, fuel margin, and flight time). Each of these functions reaches a maximum at the desired design point and has a value close to zero at the absolute constraints noted above. Starting at one end of the allowable interval, V_n is successively incremented until the other end is reached. At each increment the appropriate terminal parameters are computed, tables containing the weighting function are entered, and the overall value factor evaluated.

$$VF = f(V_{BO}, \gamma)\, g(T_F)\, h(FM, V_{BO})$$

In this manner the overall probability of success due to radar, fuel, operational considerations, and the scientific objectives can be assessed. The value $V_n = V_{n_{opt}}$ that maximizes the above product is implemented. The resulting correction is

$$\Delta V_m = \Delta V_c + V_{n_{opt}} U_3$$

Sample Results

Figures 14 and 15 present results obtained from the midcourse guidance program for selected errors in injection conditions. A vertical impact, direct ascent trajectory, with a launch azimuth of 114° arriving on July 13, 1965, was chosen for illustration. These conditions correspond to a critical late arrival-high impact velocity trajectory. The impact velocity for an arrival that corresponds to the three hour post-landing visibility constraint is 2691 m/sec, close to the maximum allowable. These conditions are critical, since any injection error will either reduce the post-landing visibility or

increase the unbraked impact velocity. Table I shows the nominal design conditions and the resulting terminal errors for perturbations in the injection velocity of ±5 m/sec. An increase of 5 m/sec in the injection velocity increases the impact velocity to 2706 m/sec or 15 m/sec above the maximum design value. A corresponding decrease in injection velocity increases the flight time so that post landing visibility is decreased by 85.7 min. The velocity in the critical plane, to correct miss only, for a midcourse maneuver 15 hours after injection, was found to be 15.3 and 13.9 m/sec, respectively.

Figure 14 shows the results of the V_n scan for the +5 m/sec case. Because of the high impact velocity, and small midcourse correction, the nominal main retro burnout velocity for the critical plane maneuver ($V_n = 0$) is 565 ft/sec, close to the maximum allowable. The fuel margin for the critical plane maneuver is 9.5 lb., or about 2.5 lb. less than that required for dispersions (Figure 6). Since the arrival time is about 20 min prior to the post landing visibility constraint, a component in the non-critical direction is used to reduce the impact velocity and the spacecraft weight. In this manner the main retro burnout velocity is decreased to a more favorable region and the fuel margin is maximized. Note that adequate post landing visibility is provided.

The above example indicates that the guidance scheme tends to maximize the fuel margin, conditioned on a reasonable burnout velocity, provided that the arrival time constraints can be met. Figure 15 is typical of the results obtained when the desired visibility cannot be achieved. The critical plane maneuver, following the -5 m/sec perturbation, reduces the post landing

visibility from Goldstone, from the desired 180 min to approximately 100 min. Note that the available fuel margin is 19.8 lb. or about 7.8 lb. more than required. This excess propellant can be used to reduce the large flight time error. A 26 m/sec component in the non-critical direction increases the post-landing visibility to 165 min, while still providing adequate propellant for terminal descent dispersions. As can be seen from the figure, any further attempt to increase the post-landing visibility reduces the probability of having sufficient propellant. The fuel margin for a miss plus flight time correction would be about 9.5 lb. or 2.5 lb. less than required.

V. CONCLUSION

The Surveyor guidance system design relies on simple mathematics based on engineering judgement. To better understand some of the simplifications of the preliminary design and to provide a more complete evaluation of system performance, a Monte-Carlo simulation of the complete mission – injection to touchdown – has been developed. The simulation employs discrete linear mapping to calculate a perturbed trajectory, but uses the complete midcourse guidance logic and contains a very accurate model of the terminal descent, based on closed form integration of the equations of motion. In this way, the combined effects of injection errors, tracking errors, midcourse execution errors, and terminal descent errors can be evaluated to provide a direct computation of probability of success. Results of this simulation for a wide variety of launch and impact conditions have shown consistently that the design procedures described here are conservative, with results showing probabilities of success generally exceeding the 0.99[1] design objective.

[1] This figure does not include reliability effects.

REFERENCES

1. Mason, M., Brainin, S. M., Descent Trajectory Optimization for Soft Lunar Landing, Aerospace Engineering 21, April 1962, pp 54-55, 82-91.

2. Noton, A. R., Cutting, E., and Barnes, F. L., Analysis of Radio Command Midcourse Guidance, JPL Tech. Rept. 32-28, September 1960.

3. Battin, R. H., A Comparison of Fixed and Variable Time of Arrival Navigation for Interplanetary Flight, Proc. 5th AFBMD/STL Aerospace Symp. Ballistic Missile Space Technology, pp 3-31, Academic Press, Inc., New York, 1960.

4. Kizner, W., A Method of Describing Miss Distances for Lunar and Interplanetary Trajectories, Ballistic Missiles and Space Technology, Vol. III, Pergamon Press, 1961.

TABLE I

NOMINAL DESIGN CONDITIONS

ARRIVAL DATE	7-13-65
ARRIVAL GMT	8 hrs. 51 min. 57 sec.
POST INJECTION FLIGHT TIME	3822.3 min.
IMPACT VELOCITY	2691. m/sec
B_T	2.39 Km
B_R	-6.6 Km

UNCORRECTED TERMINAL CONDITIONS						
INJECTION PERTURBATION	B_T Km	B_R Km	ARRIVAL VELOCITY m/sec	FLIGHT TIME Min.	GOLDSTONE POST-LANDING VISISILITY Min.	CRITICAL PLANE CORRECTION AT 15 HOURS m/sec
+5 m/sec	-1682.1	1940.3	2706	3750	252.3	15.3
-5 m/sec	1929.8	-2095.3	2673	3908	85.7	13.9

FIGURE CAPTIONS

1. Approach Geometry
2. Arrival Window and Velocity Loci
3. Range – Velocity Diagram for Vernier Descent Phase
4. Main Retro Burnout Velocity Dispersions for Inclined Approach
5. Vernier Propellant Requirement
6. Propellant Allotments for 3-σ Dispersions
7. Vernier Thrust Command Mechanization
8. Trajectory along Final Segment of Descent Contour
9. Miss Coordinates
10. Allowable Component of Midcourse Correction in Non-critical Direction
11. Fuel Margin Weighting Function
12. Burnout Velocity Weighting Function
13. Arrival Time Weighting Function for July 13, 1965.
14. Non-critical Direction Velocity Scan for a Critical Plane Correction of 15.3 m/sec and a +5 m/sec. Injection Velocity Dispersion
15. Non-critical Direction Velocity Scan for a Critical Plane Correction of 13.9 m/sec and a -5 m/sec Injection Velocity Dispersion

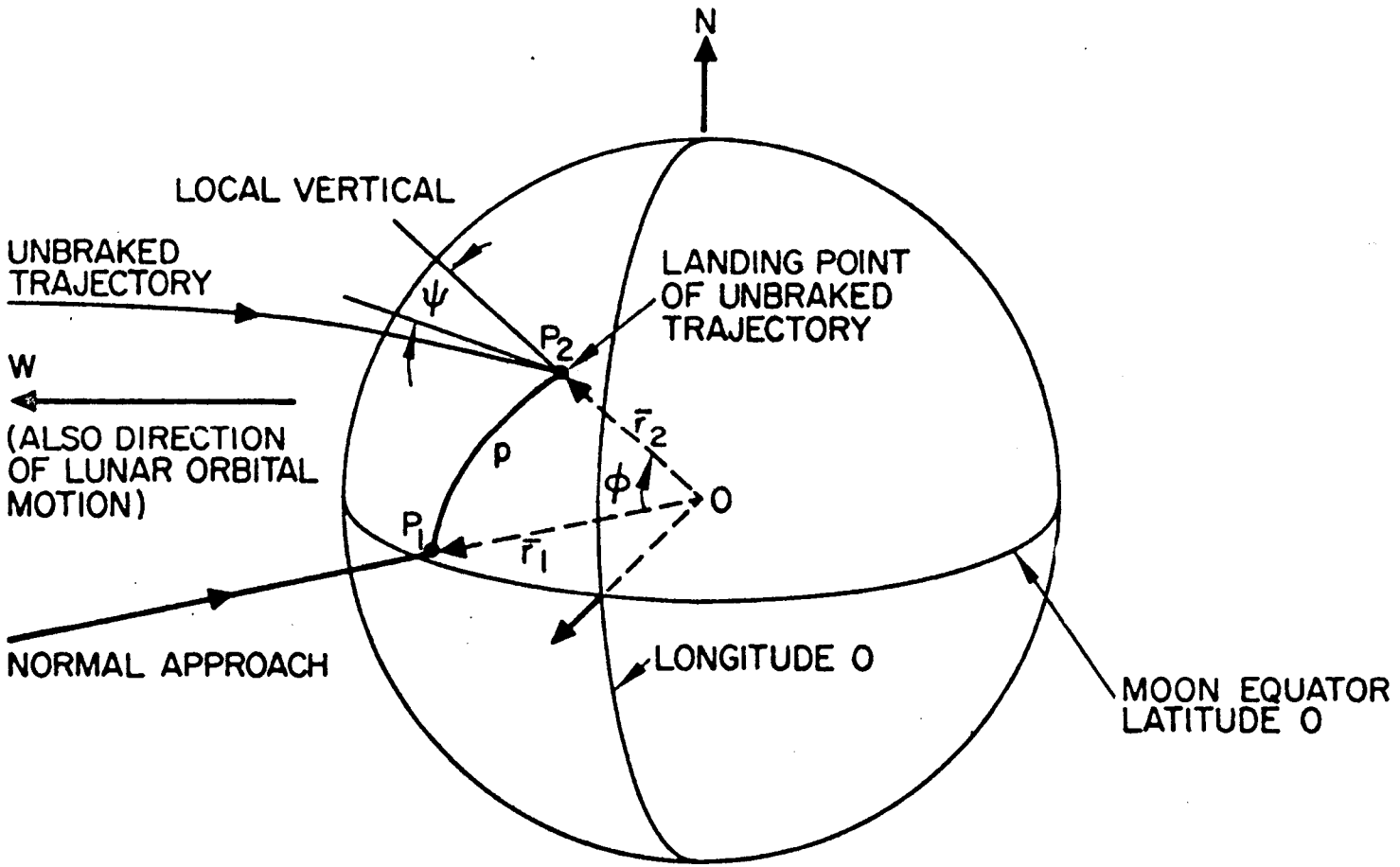

FIGURE I. APPROACH GEOMETRY

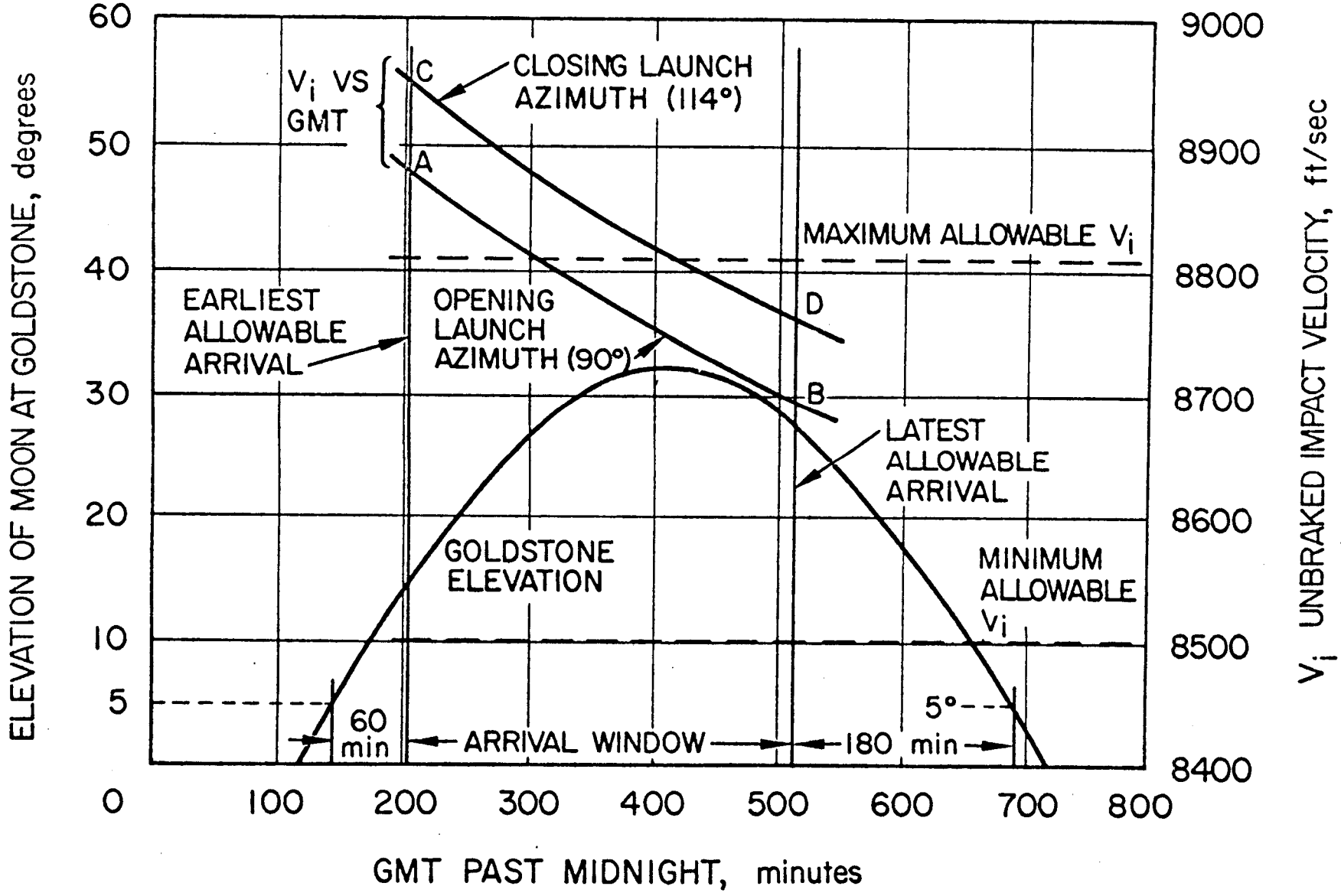

FIGURE 2. ARRIVAL WINDOW AND VELOCITY LOCI

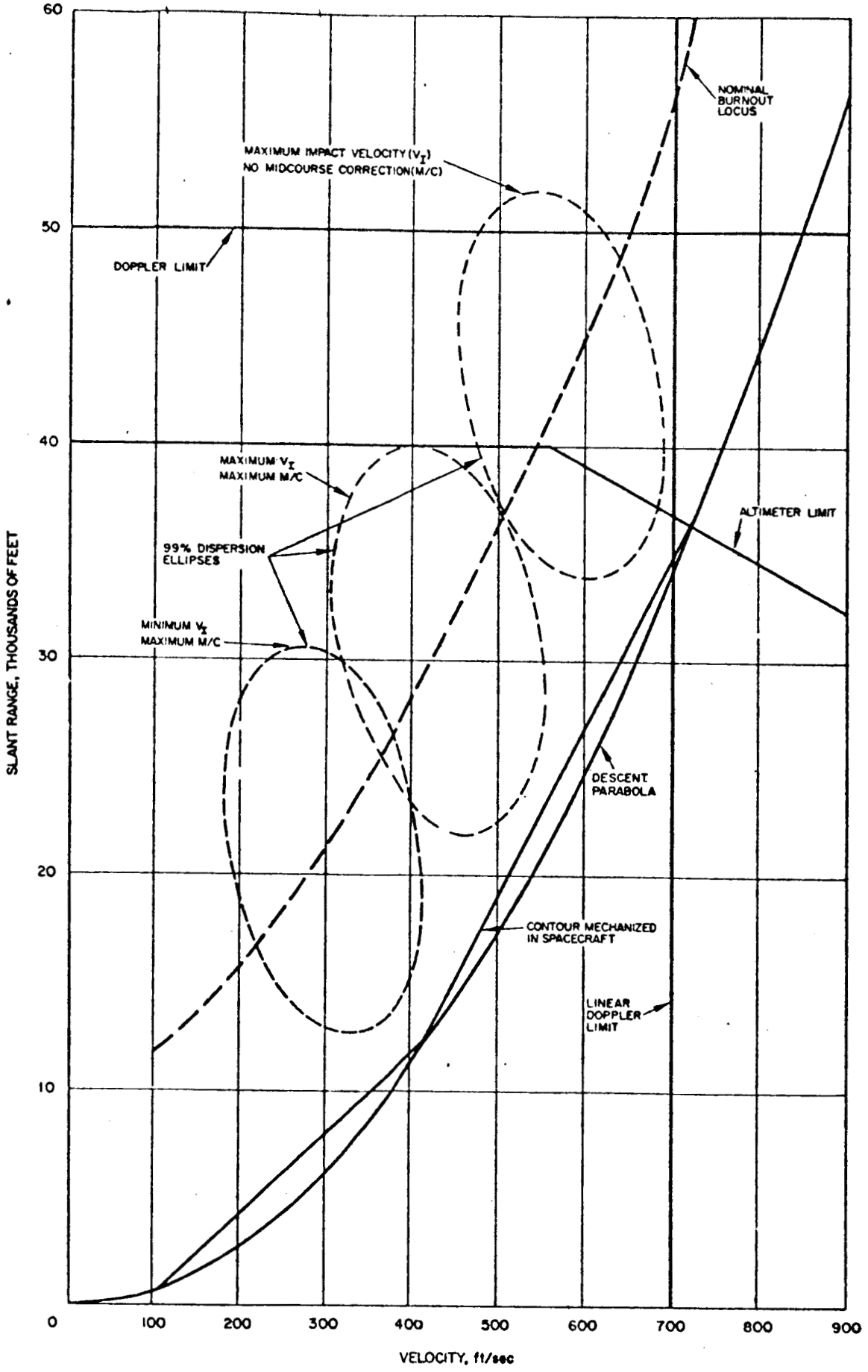

FIGURE 3. RANGE - VELOCITY DIAGRAM

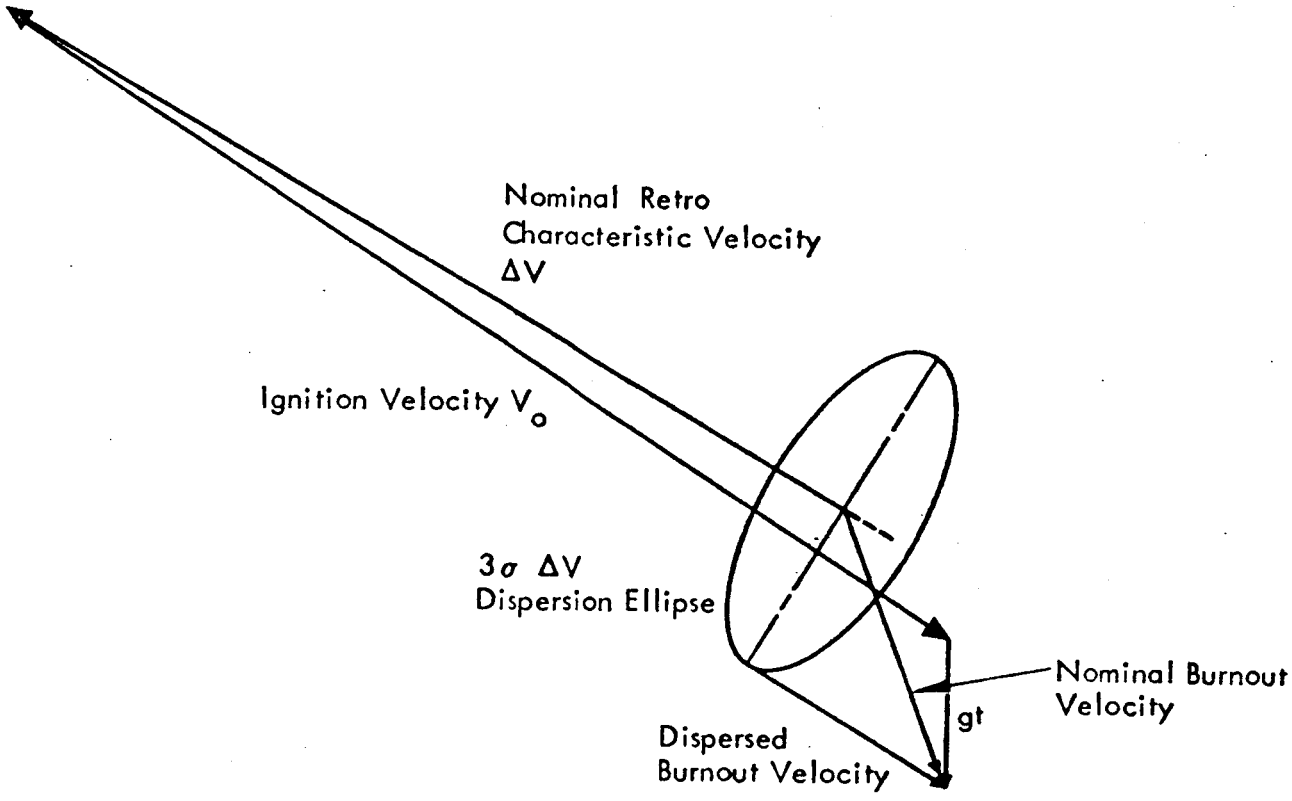

FIGURE 4. MAIN RETRO BURNOUT VELOCITY DISPERSIONS FOR INCLINED APPROACH

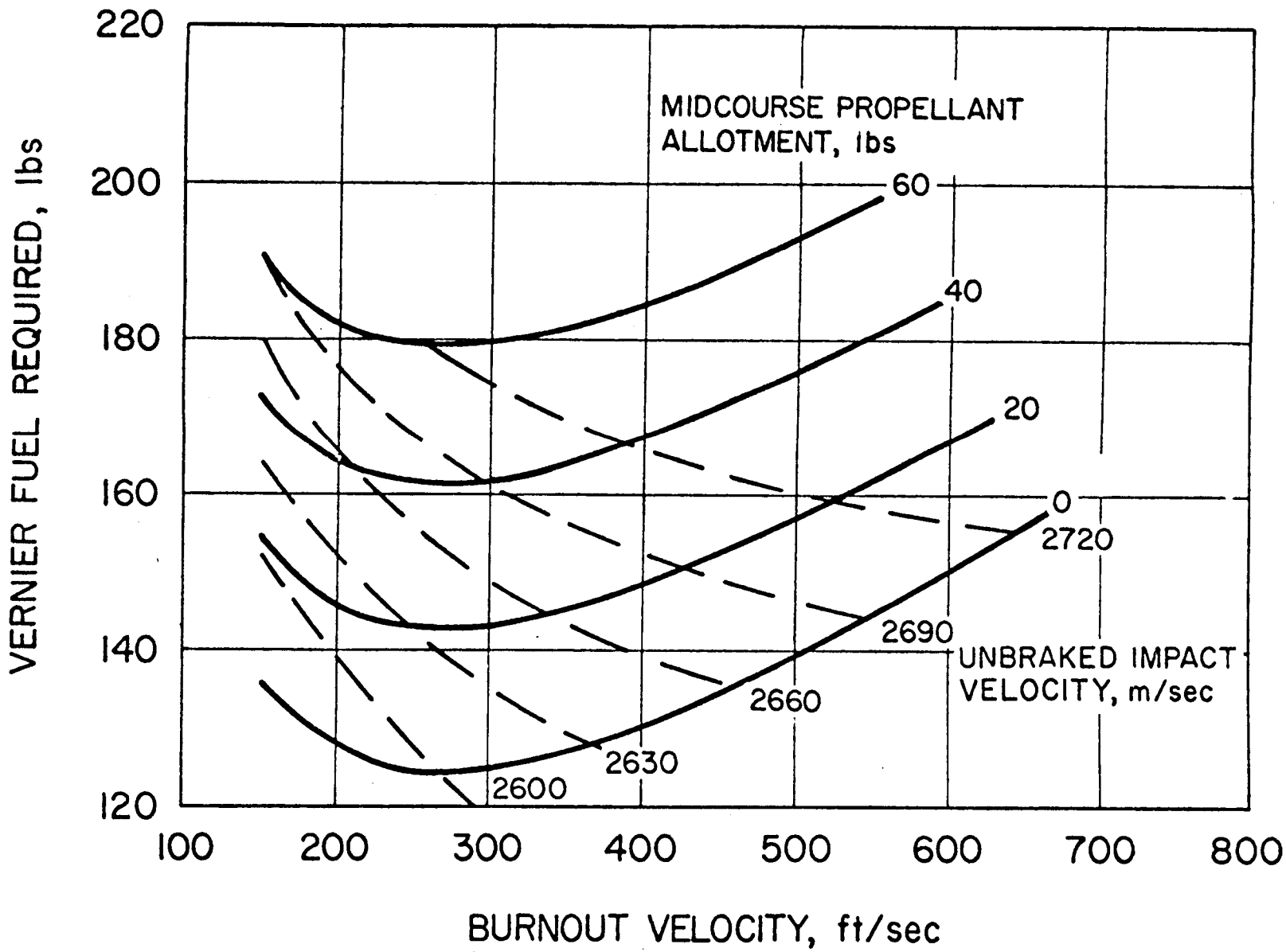

FIGURE 5. VERNIER FUEL REQUIREMENT

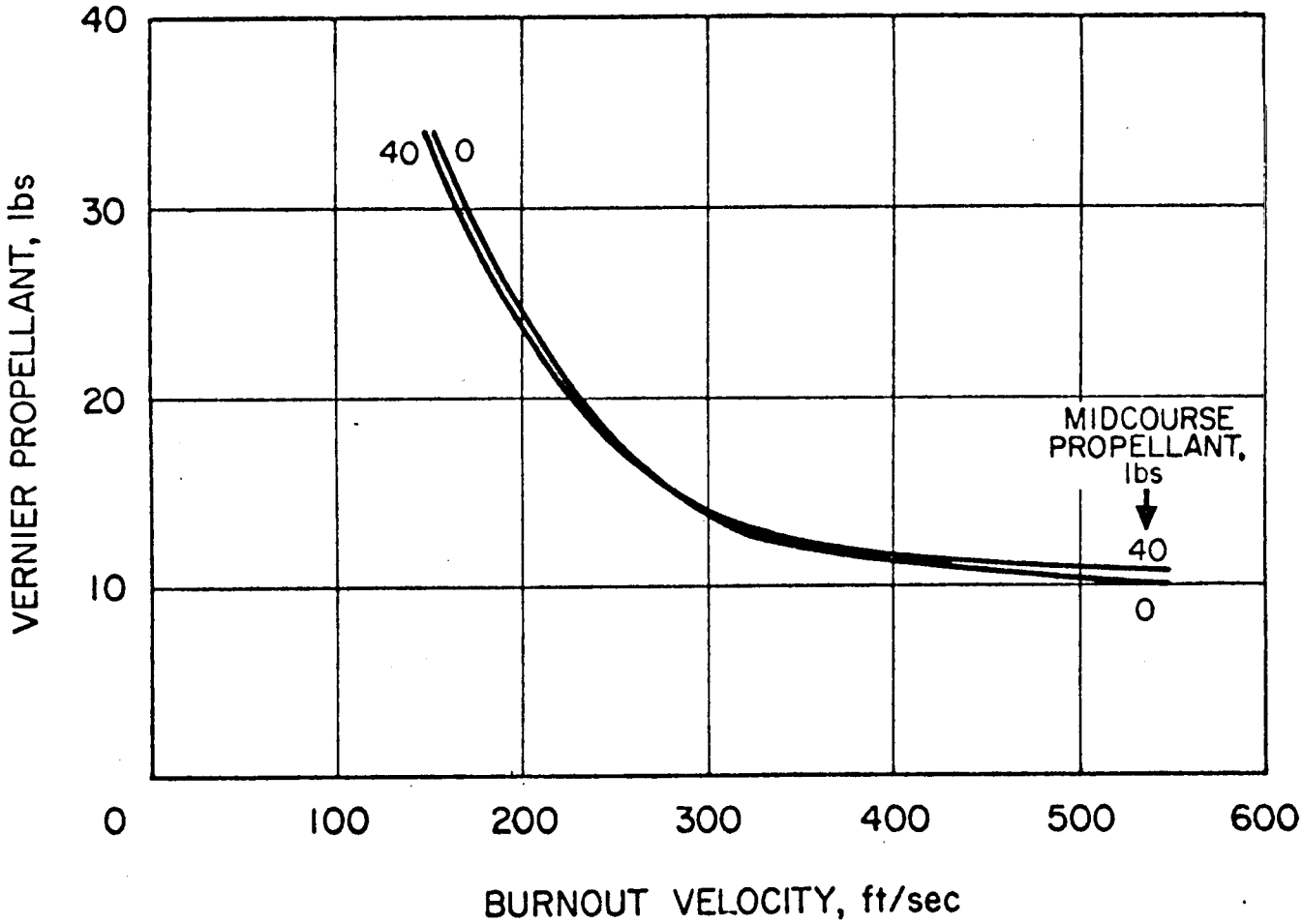

FIGURE 6. R.S.S. FUEL DISPERSIONS (3 SIGMA)

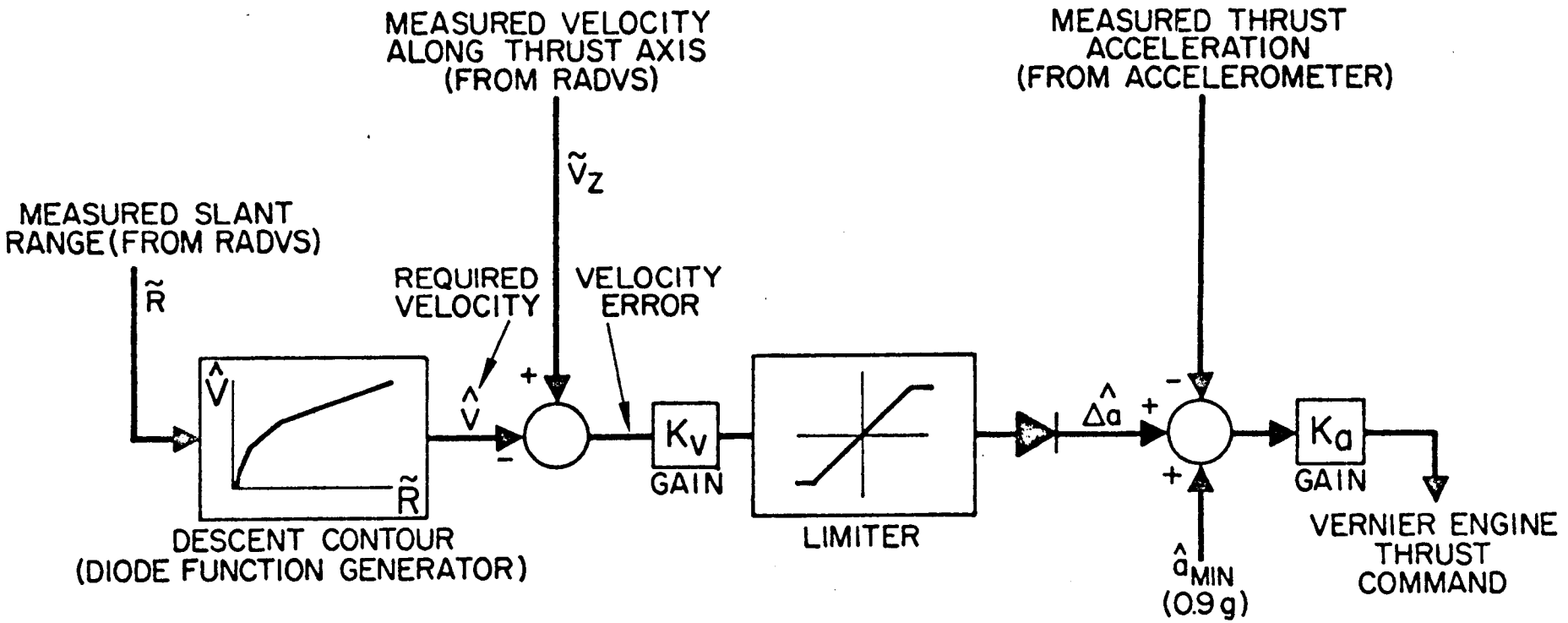

FIGURE 7. THRUST COMMAND MECHANIZATION

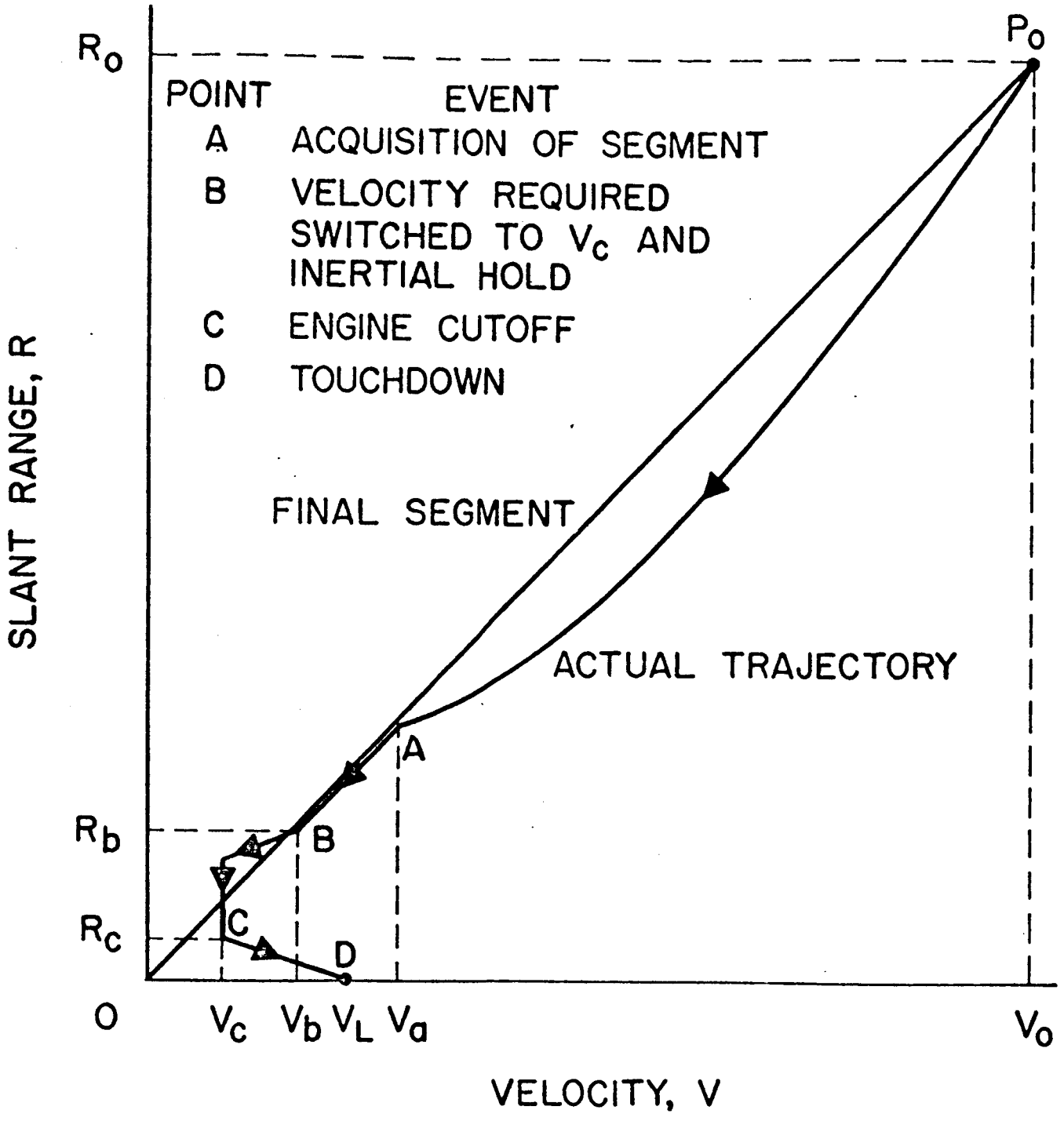

FIGURE 8. TRAJECTORY ALONG FINAL SEGMENT

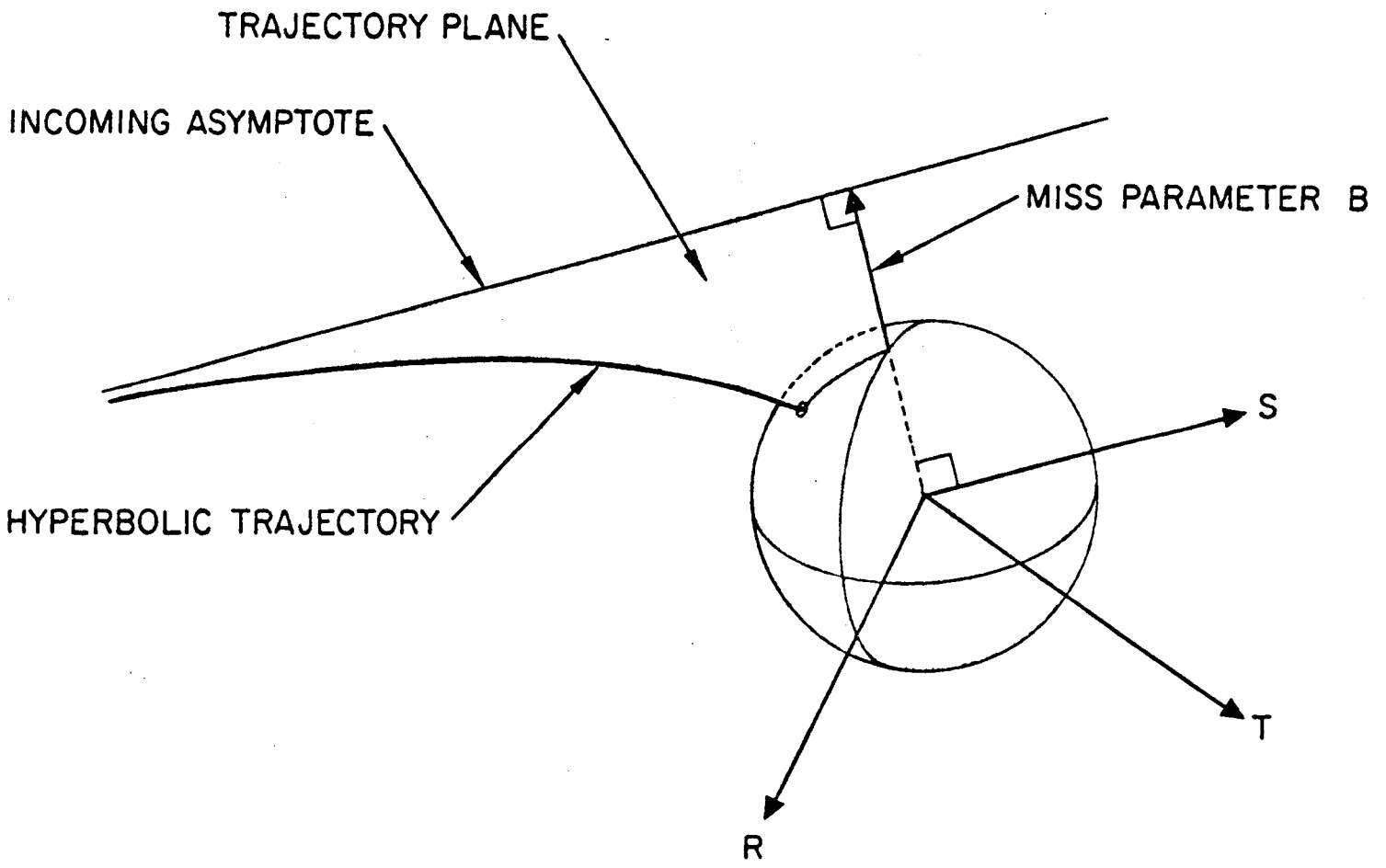

FIGURE 9. LUNAR MISS COORDINATES

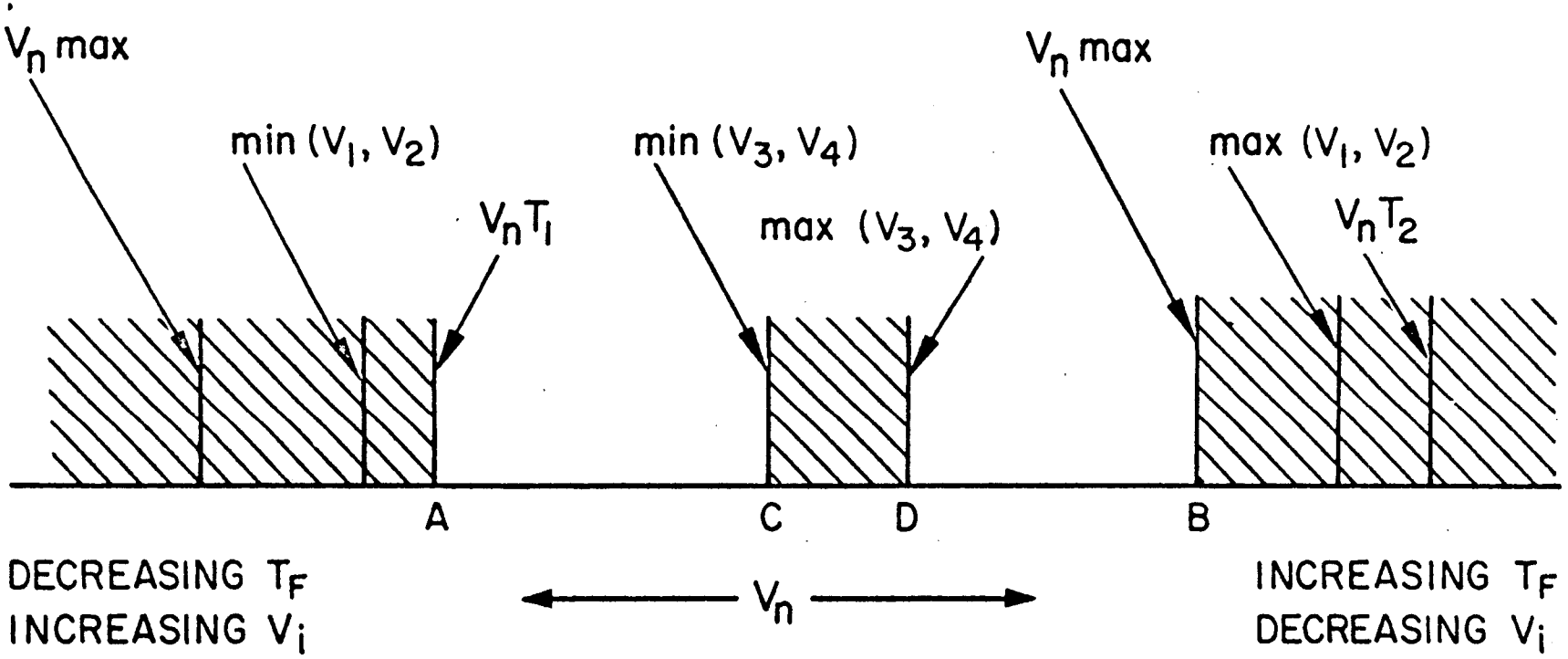

FIGURE 10. POSSIBLE NON-CRITICAL DIRECTION MIDCOURSE CORRECTIONS

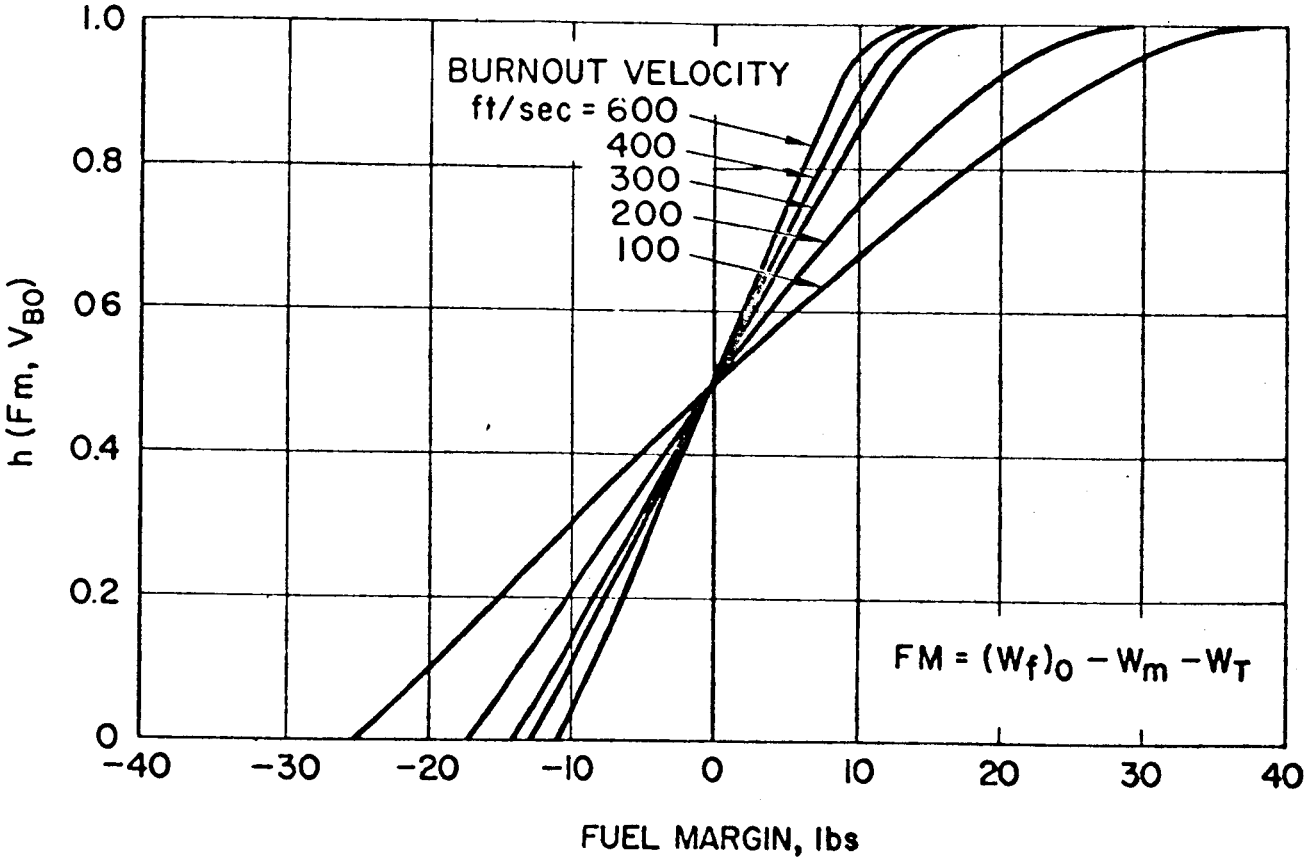

FIGURE 11. FUEL MARGIN WEIGHTING FUNCTION VS FUEL MARGIN AND MAIN RETRO BURNOUT VELOCITY

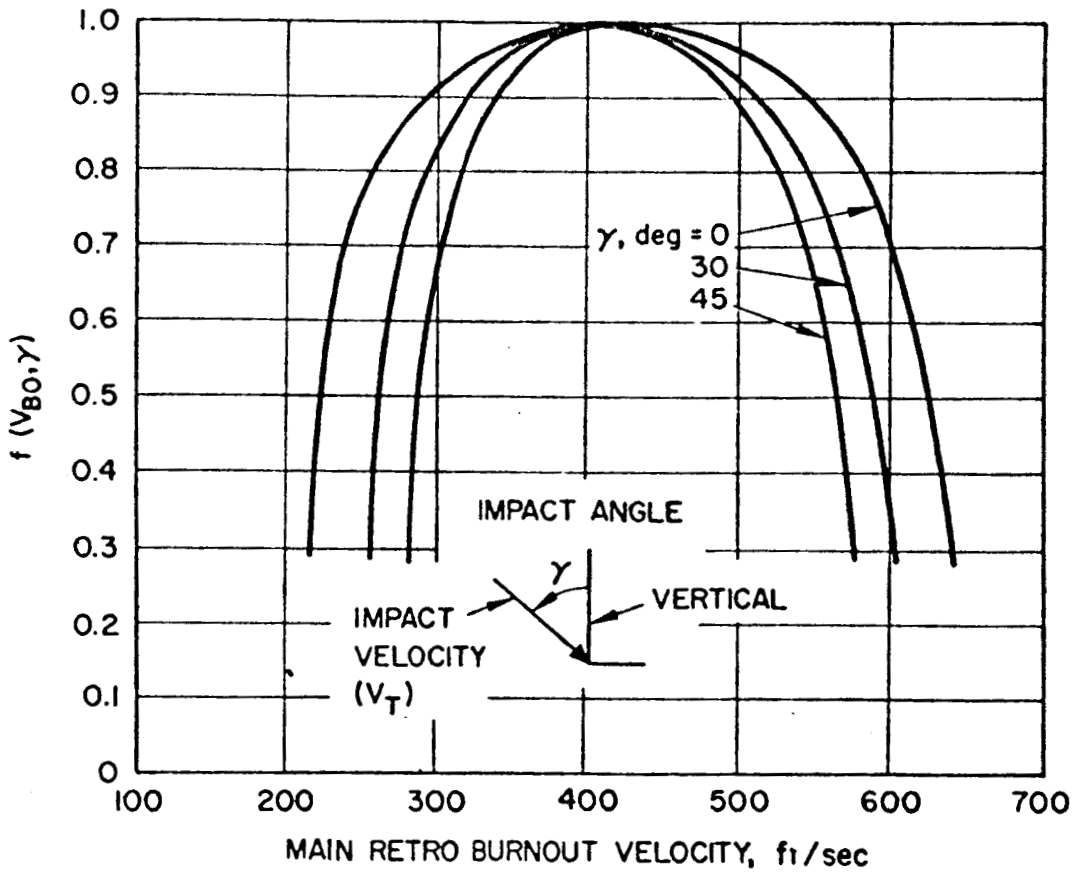

FIGURE 12. MAIN RETRO BURNOUT VELOCITY WEIGHTING FUNCTION VS BURNOUT VELOCITY AND INCIDENT ANGLE

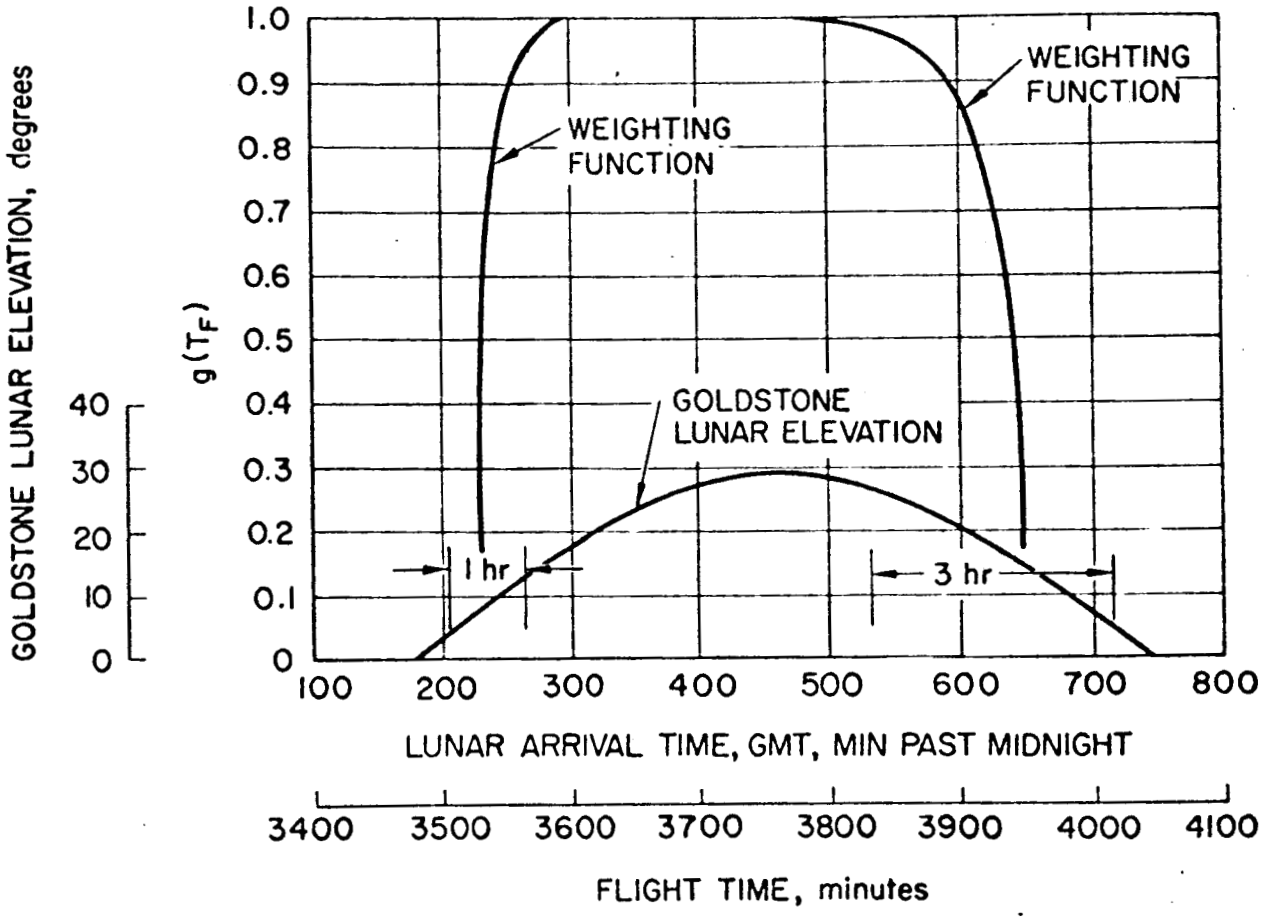

FIGURE 13. TYPICAL ARRIVAL TIME WEIGHTING FUNCTION VS ARRIVAL TIME ARRIVAL DATE JULY 13, 1965

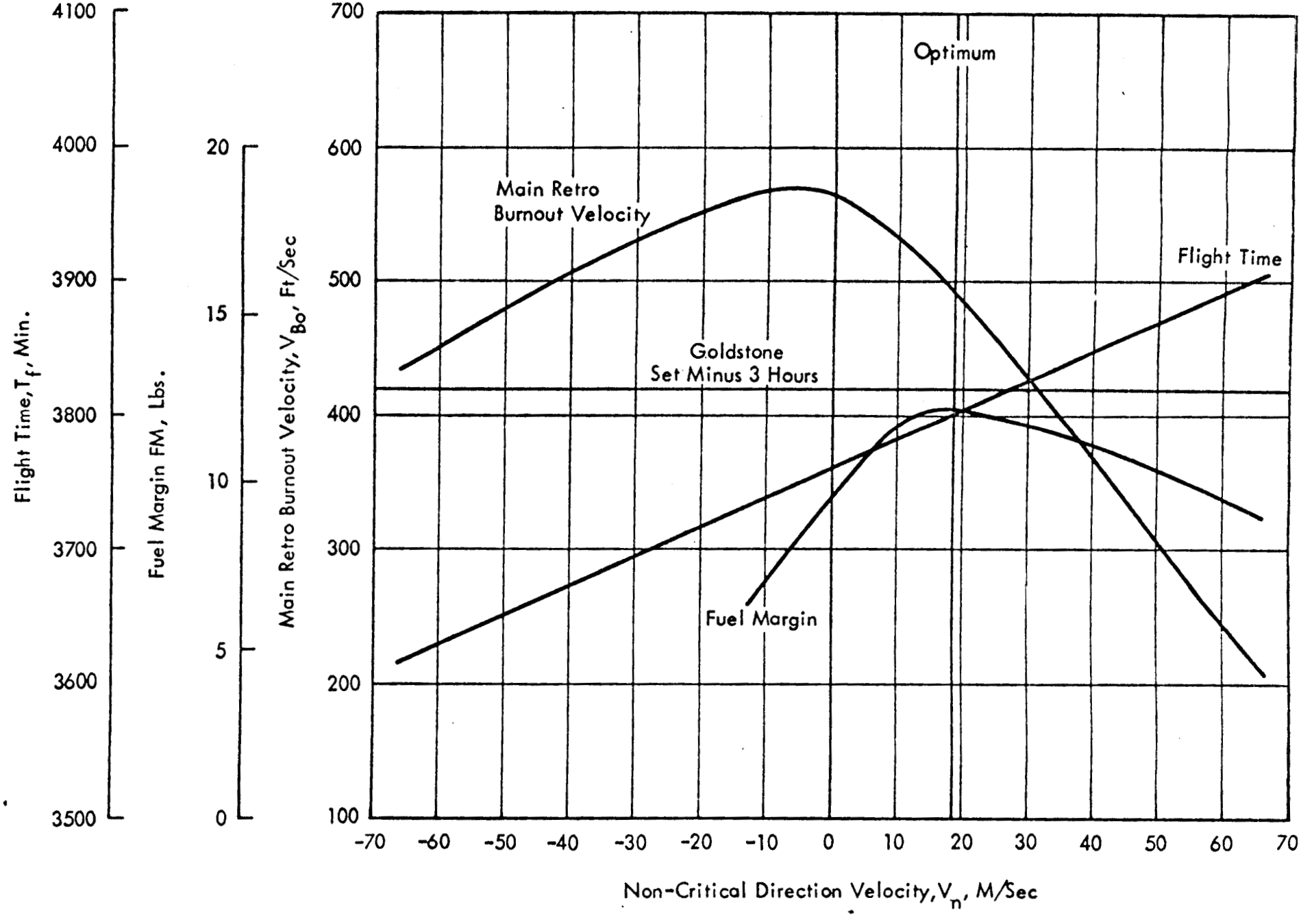

FIGURE 14. NON-CRITICAL DIRECTION VELOCITY SCAN
CRITICAL PLANE CORRECTION = 15.3 M/SEC
+5 M/SEC INJECTION VELOCITY PERTURBATION

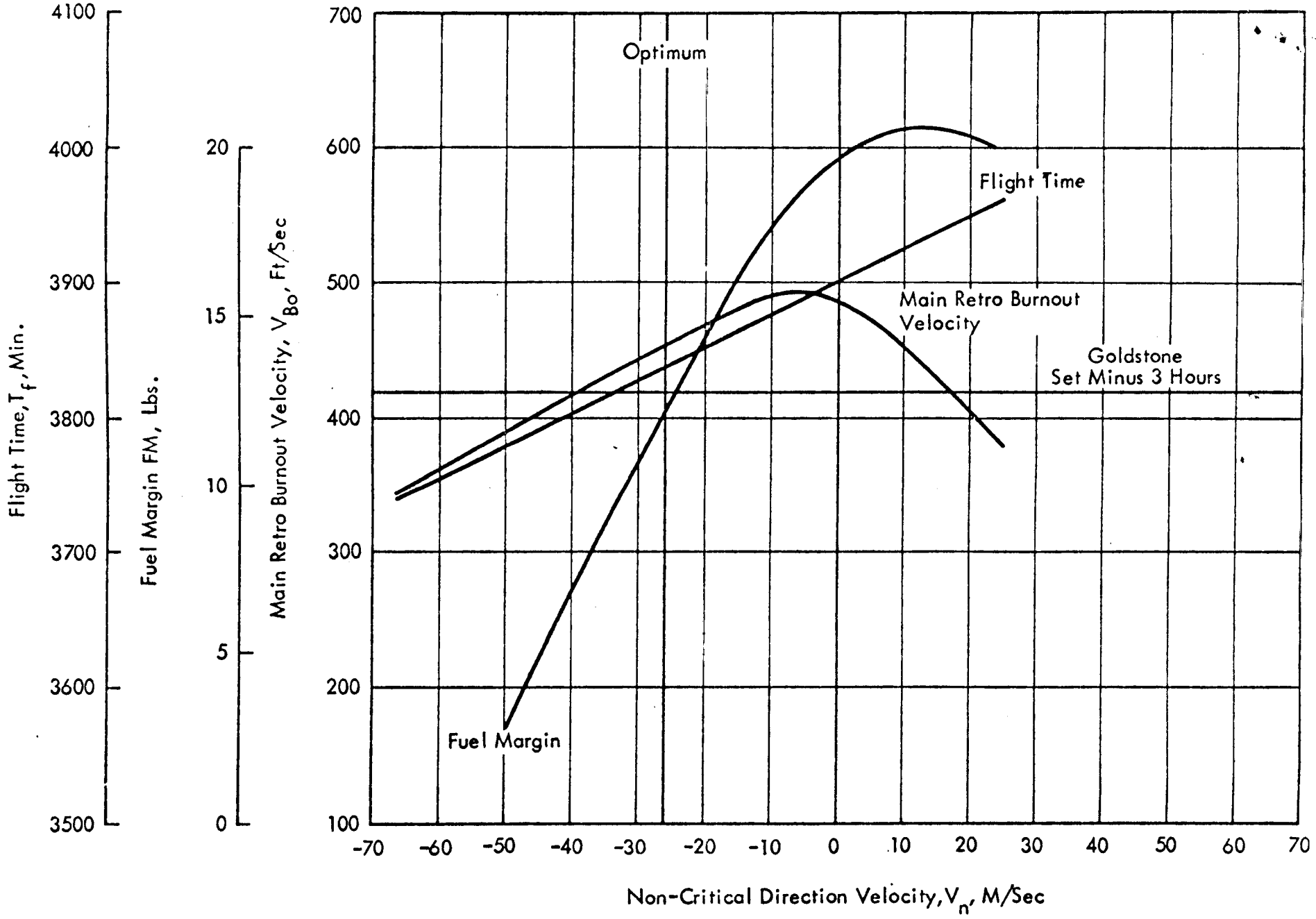

FIGURE 15. NON-CRITICAL DIRECTION VELOCITY SCAN
-5 M/SEC INJECTION VELOCITY PERTURBATION
CRITICAL PLANE CORRECTIONS = 13.9 M/SEC